Hindawi
Advances in Civil Engineering
Volume 2023, Article ID 8839774, 13 pages
https://doi.org/10.1155/2023/8839774

Research Article

Experimental Torsional Capacity of Plain Concrete Beams Made from Crushed Clay Brick and Recycled Brick Concrete as Coarse Aggregate

Md. Ashraful Alam and Syed Ishtiaq Ahmad

Department of Civil Engineering, Bangladesh University of Engineering and Technology, Dhaka 1000, Bangladesh

Correspondence should be addressed to Syed Ishtiaq Ahmad; siahmad@ce.buet.ac.bd

Received 23 June 2023; Revised 8 September 2023; Accepted 12 September 2023; Published 3 October 2023

Academic Editor: Suvash Chandra Paul

Concrete was made with four different types of coarse aggregate, i.e., natural stone aggregate concrete (NSAC), crushed virgin clay brick aggregate concrete (VBAC), crushed recycled brick concrete aggregate concrete (RBAC), and crushed recycled stone concrete aggregate concrete (RSAC). Beam specimens prepared from these four types of concrete were subjected to pure torsional moment up to failure. From this experimental procedure, ultimate torque at failure along with twisting angle were observed. From the torque vs. twisting angle curves, torsional stiffness and torsional toughness were also evaluated for these four types of concrete. It was observed that ultimate torque of VBAC and RBAC was 95% and 90% of that of NSAC, respectively. The torsional toughness of VBAC was found to be 68%–72% of that of NSAC. In addition, experimental torques were compared with predictions of torsional strength as per five commonly used models. For VBAC, the ultimate torque prediction made by skew bending theory was found to be the closest to the experimental findings.

1. Introduction

The use of alternative aggregate as opposed to natural aggregate has been on the agenda for construction companies, regulatory bodies, researchers, and academicians for the last few decades. Several investigations have been reported in the existing literature regarding the use and applicability of such materials in the building industry [1–3]. Various waste materials like concrete from old demolished buildings and structures, industrial wastes and byproducts, etc. are now being used in the production of concrete as a replacement for aggregate and supplementary cementitious material for two primary reasons: to devise ways to dispose of waste materials to promote a circular economy and to reduce burden on existing natural resources like natural aggregate as their supply is limited [4–8]. Crushed clay bricks have been used extensively in Bangladesh and adjacent areas of India for long time as natural stone is in short supply. For constructing new structures, these old brick concrete buildings are being teared down that is generating a large amount demolished concrete made from brick aggregate. Numerous studies are available in existing literature regarding the recyclability of such old brick aggregate concrete as aggregate for fresh concrete casting [9–11]. Similar studies are also available for virgin brick aggregate concrete [12–15]. It has been observed from these studies that the physical, mechanical as well as durability properties of brick and recycled brick aggregate concrete are inferior to those of natural stone aggregate concrete (NSAC) of equivalent compressive strength.

Though many aspects of mechanical properties have been studied and reported in the available literature for these two types of concrete (brick and recycled brick concrete), extensive examination of torsional behavior has not been conducted in detail. Modern analytical and design techniques with the advent of finite element based software have led to relatively smaller members, lowering conservatism that sometimes barely satisfies torsional requirements. Hence, understanding the details of torsional behavior for any type of concrete has become an important aspect of the analysis of concrete structures and structural elements. Torsional behavior for different types of plain and

reinforced normal and high-strength concrete have been examined experimentally that have been reported in the existing literature. These studies have examined effect of concrete properties as well as effect of longitudinal and transverse reinforcement on torsional behavior [16–19]. A few studies on torsional behavior of recycled stone aggregate concrete have also showed that torsional properties of such concrete are considerably inferior when 100% natural stone aggregate is replaced by the recycled aggregate [20–22]. Most of these studies employed special loading arrangement that generated pure torsional stresses in their respective beam specimens.

In line with these, a testing scheme was carried out at the Bangladesh University of Engineering and Technology to observe the comparative torsional properties of normal strength concrete made from natural stone, crushed brick, recycled brick concrete, and recycled stone as coarse aggregate. Beam specimens were prepared from these four types of coarse aggregate and were subjected to torsional load, and subsequently, their twisting pattern, failure torque, and twisting angles were observed. Information found from testing operations was analyzed and compared to get insight into the difference in torsional behavior of concrete prepared from four different types of aggregate. Further, experimental results were compared with standard torsional models widely utilized to estimate the torsional strength of concrete. This process identified the most suitable models to predict torsional strength for crushed brick and recycled brick concrete.

2. Materials and Methods

2.1. Cement and Fine Aggregate. Throughout the experimental program, ASTM Type 1 Ordinary Portland Cement that complied with the ASTM C150 [23] standard was employed as the binder. The sand used in this investigation was collected from the northeastern area of Bangladesh, which had an F.M. of 2.6, in order to make all concrete samples uniform in terms of fine aggregate. Gradation of this sand was such that it fitted within the limiting boundaries specified in ASTM C33 [24]. The fine aggregate's water absorption and specific gravity were evaluated as per ASTM C29 [25] and ASTM C128 [26], respectively, and were found to be 1.34% and 2.62, respectively.

2.2. Coarse Aggregates. Four different types of coarse aggregate, namely, natural stone aggregate (NSA), virgin brick aggregate (VBA), recycled brick concrete aggregate (RBA), and recycled stone concrete aggregate (RSA), were utilized in this work to prepare respective concrete samples. Natural crushed limestone aggregate was procured from the local market. Bangladesh standard BDS 208:2002 [27] categorizes brick into three groups. Of these three, "S" type of bricks is particularly suitable for aggregate production. Hence "S" type of brick was procured and was subsequently crushed in crusher machine to produce VBA. For the two types of recycled aggregate, two separate construction sites were selected with old buildings that were to be demolished to make way for new buildings. One of the old buildings, 37-year-old, was constructed using brick aggregate concrete, whereas, the other 23-year-old building was made of natural

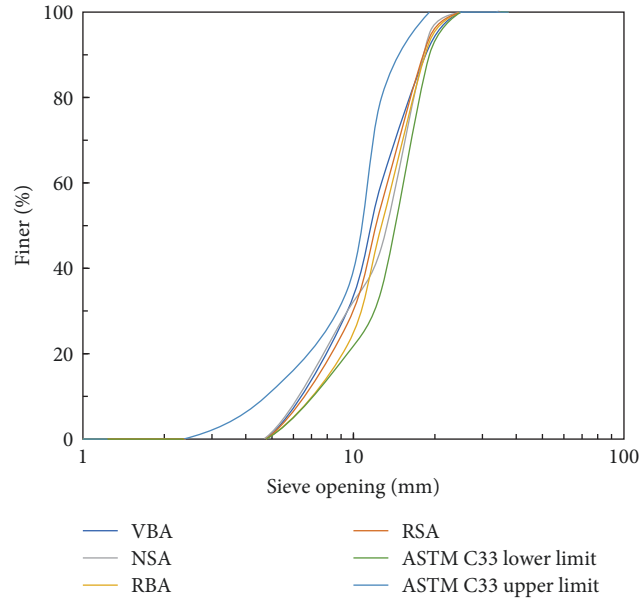

Figure 1: Gradation curves of coarse aggregates.

aggregate concrete. Concrete chunks were properly collected from these two buildings and crushed in a crusher machine. As the mechanical properties of concrete made from recycled aggregate depend on the quality of the recycled aggregate, debris, dust, and other undesirable particles were removed through careful screening [28].

In order to ensure a size distribution such that the gradation curve depicted in Figure 1 remained within the predetermined limit as set forth in ASTM C33 [24], all four types of aggregate were sieved using a 25 mm or smaller sieve. Figure 2 shows the four different types of coarse aggregate used in this experiment. Clear distinction between VBA (Figure 2(a)) and RBA (Figure 2(b) can be made because the latter's surface is obviously covered in cement mortar. Similar differences can be found between RSA (Figure 2(c)) and NSA (Figure 2(d)). The fundamental characteristics of the NSA, RSA, VBA, and RBA aggregates are shown in Table 1, along with the standard used to assess those characteristics. It is obvious from this table that NSA had higher density and substantially less water absorption capacity than that of the VBA, RBA, and RSA. The densities of VBA and RSA were found to be similar. However, RBA had much lower density, which might be caused by the aggregate particles being attached to old cement mortar [29]. Further, water absorption was found to be highest for RBA. On the other hand, it was observed that VBA's water absorption was substantially closer to the first-class brick's terminal limit as specified in BDS 202:2008 [27]. Table 1 also reports that NSA has the lowest Los Angeles (LA) abrasion value, indicating it to be the toughest of these four types of aggregates. On the other hand, RBA was found to be softer compared to the other aggregates, as its LA abrasion value was the highest. The flakiness index was also measured to give an indication of the shape of the aggregate. The flakiness index of these four different aggregates varied between a small range of 18% and 23%, demonstrating that the shapes of the aggregates were

(a) (b) (c) (d)

Figure 2: (a) VBA, (b) RBA, (c) RSA, and (d) NSA.

Table 1: Properties of coarse aggregates.

Properties	NSA	VBA	RBA	RSA
Absorption (%) ASTM C127 [30]	1.28	9.41	12.77	7.75
Fineness modulus ASTM C136 [31]	7.32	7.04	6.82	7.26
Dry rodded unit weight (kg/m^3) ASTM C127 [30]	1,523	1,218	1,122	1,227
Bulk specific gravity ASTM C127 [30]	2.58	2.32	2.14	2.35
LA Abrasion ASTM C131 [32]	21%	30%	45%	39%
Flakiness index BS812: Part 1 [33]	23%	18%	20%	22%

mostly spherical in nature. All types of coarse aggregates (NSA, VBA, RSA, and RBA) were soaked in water for 24 hr and were made saturated surface dry condition before being mixed into the concrete mixer.

3. Concrete Mix Design, Sample Preparation, and Experimental Program

Concrete samples were prepared using NSA, VBA, RSA, and RBA aggregates and are represented as NSAC, VBAC, RSAC, and RBAC, respectively. Four different water-to-cement (w/c) ratios of 0.596, 0.569, 0.527, and 0.504 were used in this work in order to produce concrete with compressive strength of 18.96 MPa (2,750 psi), 20.68 MPa (3,000 psi), 22.41 MPa (3,250 psi), and 24.13 MPa (3,500 psi) considering slump of 75–100 mm, respectively. Accordingly, concrete samples were designated both with type of coarse aggregate and target compressive strength, i.e., NSAC18.9, VBAC20.68, RBAC22.41, and so forth. The w/c ratios were on the higher side in this work since no admixture was used to achieve the desired workability of concrete as well as the range of relatively low-compressive strengths that were examined. Table 2 shows the concrete mix design ratios calculated as per American Concrete Institute (ACI) 211.1-91 [34]. Table 2 also reports the achieved slump measured as per ASTM C143 [35] and fresh density of concrete. The slump values were found to be within acceptable limits, but for VBAC and RSAC, slump values were higher compared to NSAC and RSAC. As expected, highest fresh density was found for NSAC, followed by RSAC, VBAC, and RBAC.

Beam specimens of 150 mm × 150 mm × 400 mm were prepared for evaluating torsional capacity, angle of twist, crack pattern, etc. for concrete with different coarse aggregates and different strengths. Size of beam were made to remain constant for all types of concrete to negate size effect related issues on torsional behavior of concrete [36–38]. Apart

Table 2: Mix design for concrete with different target compressive strength.

Concrete type	Target strength (MPa)	w/c	Cement (kg/m^3)	Coarse aggregate (kg/m^3)	Sand (kg/m^3)	Water (kg/m^3)	Slump (mm)	Fresh density (kg/m^3)
NSAC18.9	18.9	0.59	324	961	893	193	85	2,255
NSAC20.7	20.7	0.57	339	961	881	193	80	2,274
NSAC22.4	22.4	0.53	366	961	858	193	70	2,293
NSAC24.1	24.1	0.5	383	961	844	193	70	2,312
VBAC18.9	18.9	0.59	324	793	1,059	193	115	2,136
VBAC20.7	20.7	0.57	339	793	1,046	193	110	2,155
VBAC22.4	22.4	0.53	366	793	1,024	193	80	2,174
VBAC24.1	24.1	0.5	383	793	1,010	193	75	2,184
RSAC18.9	18.9	0.59	324	799	1,053	193	95	2,212
RSAC20.7	20.7	0.57	339	799	1,040	193	100	2,231
RSAC22.4	22.4	0.53	366	799	1,018	193	75	2,250
RSAC24.1	24.1	0.5	383	799	1,004	193	75	2,269
RBAC18.9	18.9	0.59	324	731	1,121	193	125	2,117
RBAC20.7	20.7	0.57	339	731	1,108	193	115	2,126
RBAC22.4	22.4	0.53	366	731	1,085	193	110	2,145
RBAC24.1	24.1	0.5	383	731	1,072	193	80	2,184

from this, nine-cylinder specimens (100 mm × 200 mm) were also prepared for evaluating the compressive strength, splitting tensile strengths, and density void ratios of each type of concrete. All specimens were cured by immersion in water for 28 days before they were subjected to respective testing. Table 3 shows a tally of the concrete specimens that were used in this experimental program. Altogether, a total of 160 specimens were used in this work.

3.1. Experimental Setup. Figure 3(a) shows beam specimens (150 mm × 150 mm × 400 mm) being loaded at their diagonally opposite ends with steel I joists (painted in red) on the top surface. The load was applied through a column fixed at the center of this joist. This column was attached to a universal testing machine (Brand: Shimadzu; Capacity 1,000 tons) that applied loads in displacement control mode. From the I joist, load was transferred to the concrete beam through spherical balls. Again, these spherical balls rested on stainless steel bearing plates (37.5 mm × 37.5 mm × 6 mm) that were attached to the beam surface using epoxy (Figure 3(b)). Figure 3(a) also shows a laser displacement sensor in front of the beam specimen that recorded the specimen's displacement.

At the center zone of the beam, this opposing load application and support system produced pure torsion. In order to avoid indeterminacy and prevent the generation of axial forces, one spherical ball was allowed to roll in both directions while the other ball had the ability to roll in the transverse direction only. The experimental procedure followed here is in line with that followed by Bažant et al. [36].

3.2. Sensor, Device, and Software Setup for Torsional Test. The load was applied at the midpoint of the I joist under displacement control regime, which transmitted the load equally at the two diagonal ends of the top surface of the beam. As the support at the beam bottom surface was on two opposite diagonal ends, this special arrangement created a pure torsional moment in the beam by creating opposite movement at all four ends of the beam. Four laser displacement measurement sensors were used at four different sides of the specimen, as shown in Figure 4, to capture this displacement. Specification of the sensor was, Laser Radiation, Maximum Output (peak): 1.2 Mw, Pulse Duration: 22 ms, Wavelength: 650 mm, Class 2 Laser Product, satisfying EN 60825-1:2007. Magnetic stands were used to mount the laser sensor so that it could be positioned wherever it was most appropriate. The displacement of the beam was determined using Lab View software [42]. The data collector (NI USB-6211, 16 inputs, 16 bits, 250 KS/s, multifunction) device collected the signal from the laser displacement measurement device and sent it to the lab view software. These measured displacements were processed to determine the rotation of the beam. The laser displacement sensor, data collector, and necessary power input devices are shown in Figure 5.

4. Results and Discussion

4.1. Compressive and Splitting Tensile Strength. The 28-day compressive and splitting tensile strengths for each kind of concrete are shown in Table 4. The achieved compressive strength was only somewhat greater than the target strength for the case of NSAC. For the remaining three, i.e., VBAC, RSAC, and RBAC, the observed compressive strength at 28^{th} was lower than the target strength. The LAA test showed that VBA, RBA, and RSA are relatively softer than NSA (Table 1); as a result, using the ACI code mix design approach had difficulties in reaching target strength for concrete prepared from these aggregates [9, 12–14]. The physical characteristics of each form of concrete, including density, porosity, and absorption, are listed in Table 5. This table shows that NSAC and RSAC have the highest apparent and bulk densities, followed by VBAC and RBAC. In contrast to NSAC and RSAC, voids and absorption were much higher in RBAC and VBAC.

Table 3: List of specimens and testing program.

Test name and method	Shape and size of specimen (mm)	Compressive strength (MPa)	Number of specimens				Total specimen
			NS	VB	RS	RB	
Compressive strength ASTM C39 [39]	Cylinder Ø 100 × 200	18.9	3	3	3	3	48
		20.7	3	3	3	3	
		22.4	3	3	3	3	
		24.1	3	3	3	3	
Tensile strength ASTM C496 [40]	Cylinder Ø 100 × 200	18.9	3	3	3	3	48
		20.7	3	3	3	3	
		22.4	3	3	3	3	
		24.1	3	3	3	3	
Density/absorption ASTM C642 [41]	Cylinder Ø 100 × 200	18.9	3	3	3	3	48
		20.7	3	3	3	3	
		22.4	3	3	3	3	
		24.1	3	3	3	3	
Torsional parameters	Beam 150 × 150 × 400	18.9	2	2	2	2	32
		20.7	2	2	2	2	
		22.4	2	2	2	2	
		24.1	2	2	2	2	
					Total =		176

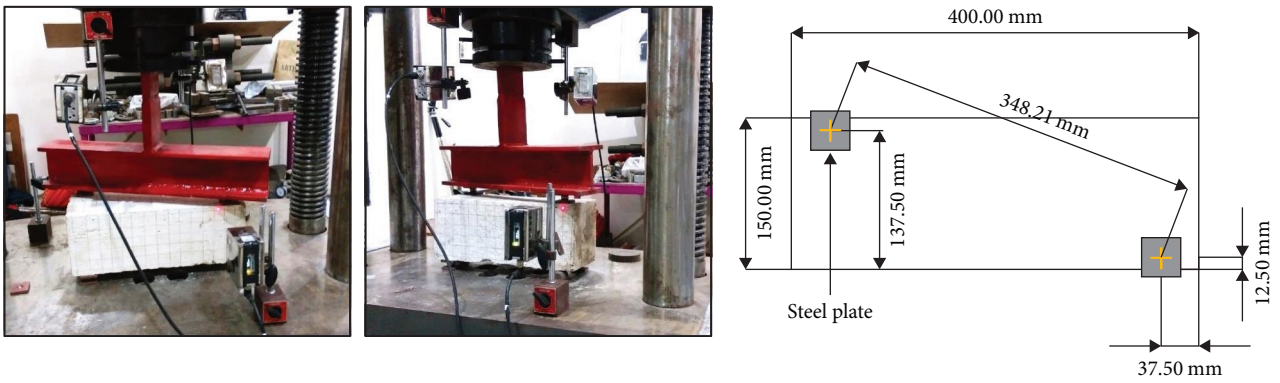

Figure 3: Configuration of torsional test setup (a) beam loaded with steel I joist and (b) steel plate attached at top and bottom surface to support spherical balls.

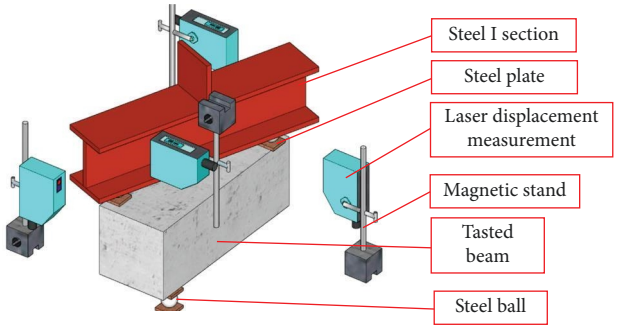

Figure 4: 3D view of torsion test setup.

4.2. Torsional Parameters. The average torsional properties obtained from the two tested beams for each case are reported in Table 6. According to the results for a given target strength, NSAC had the highest ultimate torque, followed by VBAC, RSAC, and RBAC. In the case of VBAC, ultimate torque was around 95% of that of NSAC. The ultimate torque of RSAC ranged between 92% and 93% of that of NSAC. RBAC's ultimate torque was significantly lower, ranging from 87% to 90% of that of NSAC. Taking into account the sample size and concrete compressive strength, the torsional capacity observed for NSAC in this study was found to be equivalent to that reported in the existing literature [21, 43]. The twisting angle at ultimate torque changed with torque, i.e., the larger the twisting angle, the greater the torque. While preparing concrete with a specific target compressive strength, all parameters were kept constant except the coarse aggregate. Hence, the difference in ultimate torque for NSAC, VBAC, RSAC, and RBAC was clearly related to changes in coarse aggregate characteristics. Table 1 shows that VBA is substantially softer, has a higher LAA value, and is more porous than NSA. As a result,

(a) (b) (c)

(d) (e)

Figure 5: (a–c) Side, back, and top view of laser displacement sensor, respectively. (d) data acquisition device and (e) power supply controller of laser displacement sensor.

VBAC's torsional properties were found to be inferior to those of NSAC. Similar reasonings applied to concrete with recycled aggregates, i.e., RSAC and RBAC.

Figure 6(a)–6(d) shows the torque vs. twisting angle diagram up to failure for all the beams tested in this experimental scheme. Two distinctive behaviors of torque versus twisting curves was observed from these figures. For NSAC and RSAC, torque versus twisting angle curves had a steeper initial slope that progressively became flatter as it approached failure. Though RSA is softer than NSA due to the preexistence of microcracks as evident from LAA value (Table 1), the torque vs. twisting graph was found to be similar for NSAC and RSAC. This was probably due to the fact that residual cementing properties and better interlocking due to preexisting microcracks in RSA enhanced the overall stiffness of RSAC. In contrast, for brick aggregate concretes, i.e., both VBAC and RBAC, the initial slope of torque vs. twisting angle was much flatter compared to stone (both NSAC and RSAC) aggregate concrete. After the initial zone, the slope of the torque vs. twisting curve for VBAC and RBAC abruptly increased and stayed quite steady up to the failure zone. At close to failure, the slope of the torque vs. twisting curve for VBAC and RBAC decreased rapidly, and the curve became much flatter. The initial slope in VBAC and RBAC was lower due to the initiation and progression of microcracks at a much lower stress level than that for NSAC. Another reason may be that the porosity, voids and absorption in VBAC and RBAC are much higher than those in NSAC (Table 4). At initial stages of loading, filling up of these voids due to applied stresses might have taken place that reduced the stiffness. After a sufficient portion of voids were rearranged and filled due to applied stresses, the stiffness started to increase again. The increase in stiffness afterward might also be due to the interlocking action between the rough internal crack surfaces.

Table 4: Mechanical properties of NSAC, VBAC, RSAC, and RBAC.

Concrete type	Compressive strength (MPa)	SD	Tensile strength (MPa)	SD
NSAC18.9	19.8	0.267	2.2	0.063
NSAC20.7	21.6	0.350	2.6	0.120
NSAC22.4	23.5	0.398	2.9	0.087
NSAC24.1	25.5	0.407	3.5	0.125
VBAC18.9	17.8	0.594	1.8	0.103
VBAC20.7	19.4	0.967	2.0	0.100
VBAC22.4	21.0	0.822	2.2	0.161
VBAC24.1	22.5	0.929	2.5	0.133
RSAC18.9	17.7	0.386	1.8	0.016
RSAC20.7	19.2	0.403	1.9	0.065
RSAC22.4	20.7	0.368	2.2	0.069
RSAC24.1	22.2	0.616	2.4	0.102
RBAC18.9	17.4	0.785	1.7	0.056
RBAC20.7	19.0	0.946	1.9	0.091
RBAC22.4	20.4	1.208	2.1	0.132
RBAC24.1	21.9	1.744	2.3	0.147

Note: SD: standard deviation.

Table 5: Physical properties of NSAC, VBAC, RSAC, and RBAC.

Concrete type	Bulk density (Mg/m^3)	SD	Apparent density (Mg/m^3)	SD	Porosity (%)	SD	Absorption	SD
NSAC18.9	2.130	0.002	2.350	0.003	8.900	0.010	4.100	0.005
NSAC20.7	2.150	0.001	2.340	0.001	8.400	0.005	3.800	0.002
NSAC22.4	2.150	0.002	2.330	0.002	8.050	0.006	3.700	0.003
NSAC24.1	2.170	0.003	2.320	0.003	7.400	0.009	3.250	0.004
VBAC18.9	1.820	0.006	2.100	0.006	11.700	0.036	6.200	0.019
VBAC20.7	1.840	0.009	2.090	0.010	11.300	0.055	5.980	0.029
VBAC22.4	1.850	0.005	2.080	0.006	10.500	0.030	5.600	0.016
VBAC24.1	1.870	0.012	2.070	0.014	9.850	0.066	5.100	0.034
RSAC18.9	1.960	0.008	2.290	0.009	11.010	0.045	5.700	0.023
RSAC20.7	1.970	0.023	2.280	0.027	10.300	0.122	5.300	0.063
RSAC22.4	1.970	0.022	2.280	0.026	9.800	0.111	5.100	0.058
RSAC24.1	2.000	0.025	2.270	0.028	9.210	0.115	4.700	0.059
RBAC18.9	1.780	0.020	2.070	0.024	15.550	0.178	8.600	0.099
RBAC20.7	1.790	0.025	2.060	0.029	14.800	0.206	8.150	0.113
RBAC22.4	1.800	0.041	2.050	0.047	14.300	0.326	7.850	0.179
RBAC24.1	1.810	0.074	2.040	0.083	13.200	0.537	7.200	0.293

Note: SD: standard deviation.

Table 5 lists the initial stiffness of all types of concrete, from which it can be seen that for VBAC and RBAC, the initial stiffness was only 47%–52% of that of NSAC. Although VBAC had a lower initial slope than RSAC, ultimate torque was always higher in VBAC.

Additionally, Table 6 provides information on the torsional toughness, i.e., the energy absorbed up to torsional failure for concrete made from different types of coarse aggregates. As can be seen, VBAC had a torsional toughness of 68%–72% of that of NSAC. Whereas, the torsional toughness of RBAC was only about 58%–61% of that of NSAC. Torsional toughness for RSAC, on the other hand, was between 84% and 88% of that of NSAC. The torque vs. twisting diagram (Figure 6(a)–6(d)) reveals that for the cases of VBAC and RBAC, the initial torsional rigidity was much lower, resulting in torque vs. twisting curves that had substantially smaller areas under them, i.e., absorbed energy was much less for the case of VBAC and RBAC. On the basis of this, it can be concluded that concrete built with VBA and RBA requires significantly less energy to fail in torsion.

4.3. Crack Pattern. Figure 7 shows a three-dimensional schematic diagram of a beam with a failure crack, along with the location and orientation of the cracks. The crack angle after

Table 6: Torsional properties of NSAC, VBAC, RSAC, and RBAC.

Concrete type	Target strength (MPa)	Ultimate torque (kN m)	Twist at ultimate torque (rad/m)	Initial torsional stiffness (kN m^2)	Torsional toughness (kN m/m)
NSAC18.9	18.9	2.731	5.06E-03	698.086	8.06E-03
NSAC20.7	20.7	2.893	5.14E-03	797.431	8.86E-03
NSAC22.4	22.4	3.062	5.23E-03	871.159	9.73E-03
NSAC24.1	24.1	3.201	5.36E-03	928.424	1.05E-02
VBAC18.9	18.9	2.592	4.82E-03	361.139	5.54E-03
VBAC20.7	20.7	2.734	4.97E-03	372.872	6.26E-03
VBAC22.4	22.4	2.879	5.08E-03	448.18	7.09E-03
VBAC24.1	24.1	3.024	5.13E-03	484.129	7.63E-03
RSAC18.9	18.9	2.554	4.79E-03	632.642	6.84E-03
RSAC20.7	20.7	2.685	4.93E-03	723.144	7.72E-03
RSAC22.4	22.4	2.831	4.98E-03	828.816	8.54E-03
RSAC24.1	24.1	2.967	5.08E-03	880.775	9.24E-03
RBAC18.9	18.9	2.482	4.61E-03	294.861	4.72E-03
RBAC20.7	20.7	2.594	4.74E-03	320.179	5.26E-03
RBAC22.4	22.4	2.716	4.81E-03	391.744	5.91E-03
RBAC24.1	24.1	2.793	4.89E-03	420.311	6.36E-03

failure was measured for all beams. Pure torsion creates biaxial compression–tension situation along diagonal directions that cause failure at around 45° crack angles [44]. Figure 8 shows crack orientation with distance from the corresponding end for all cracks. From this figure, it can be seen that for NSAC beams, failure angles varied between 44.3° and 46.5°. For VBAC beams, the failure angle was found to be to varied between 43° and 56.5°. Whereas, for RSAC beams, the failure angle was between 44.2° and 46.2°, and for RBAC beams, the failure angle had a large variation between 39.2° and 56.9°, respectively. As can be seen, for NSAC and RSAC, the angle of the crack is close to 45°, but for VBAC and RBAC, the range of variation of the crack angle was much higher. Greater variation in the crack angles for VBAC and RBAC compared to NSAC and RSAC possibly caused by the presence of more microdefects and increased porosity in VBA and RBA compared to NSA and RSA.

Figure 9 shows typical crack surfaces for NSAC and VBAC beams. It may be observed that the crack surface of the VBAC beam is comparatively smoother than that of the NSAC beam, which is irregular with protruding aggregates over the surface.

5. Result Comparison with Different Theories and Codes

Torsional behavior of concrete made different coarse aggregate were next compared with the available torsional strength model. Five widely used models, i.e., elastic theory [45, 46], plastic theory [46, 47], ACI code method [48], Turkish standard TS500 [49], and Skew bending theory [50] were examined for this purpose.

According to elastic theory, which is from St. Venant's principle, torsional capacity of plain concrete member is expressed as follows:

$$T = \alpha x^2 y^* f_t, \tag{1}$$

where T = failure torque, kN m;

f_t = tensile strength of concrete, MPa;

x, y = length of short and long sides of the section, respectively;

α = a coefficient with values ranging from 0.208 to 0.333 and dependent on y/x ratios. Since, in the present experimental configuration, $y/x = 1$, the value of α was taken as 0.208 [45].

Plastic theory incorporates concrete properties in the plastic range. Likewise in the elastic theory, failure is considered when the maximum principal tensile stress becomes equivalent to tensile strength of concrete, f_t. The failure torque following plastic theory is expressed as per following equation:

$$T = \left(0.5 - \frac{x}{6y}\right)(x^2 y)\left(6\sqrt{f_c'}\right). \tag{2}$$

ACI adopted space truss analogy and according to ACI 318-19, torsional strength (cracking torque) is given by:

$$T = 4\lambda\sqrt{f_c'}\frac{A_{Cp}^2}{P_{Cp}}. \tag{3}$$

A_{cp} = area bounded by external concrete cross-sectional perimeter, mm^2;

P_{cp} = perimeter of concrete cross-section, mm. For this experimental scheme, since normal weight concrete was used, λ was taken as 1.

Cracking or failure torque T as per Turkish Standard (TS500) is calculated from the following equation:

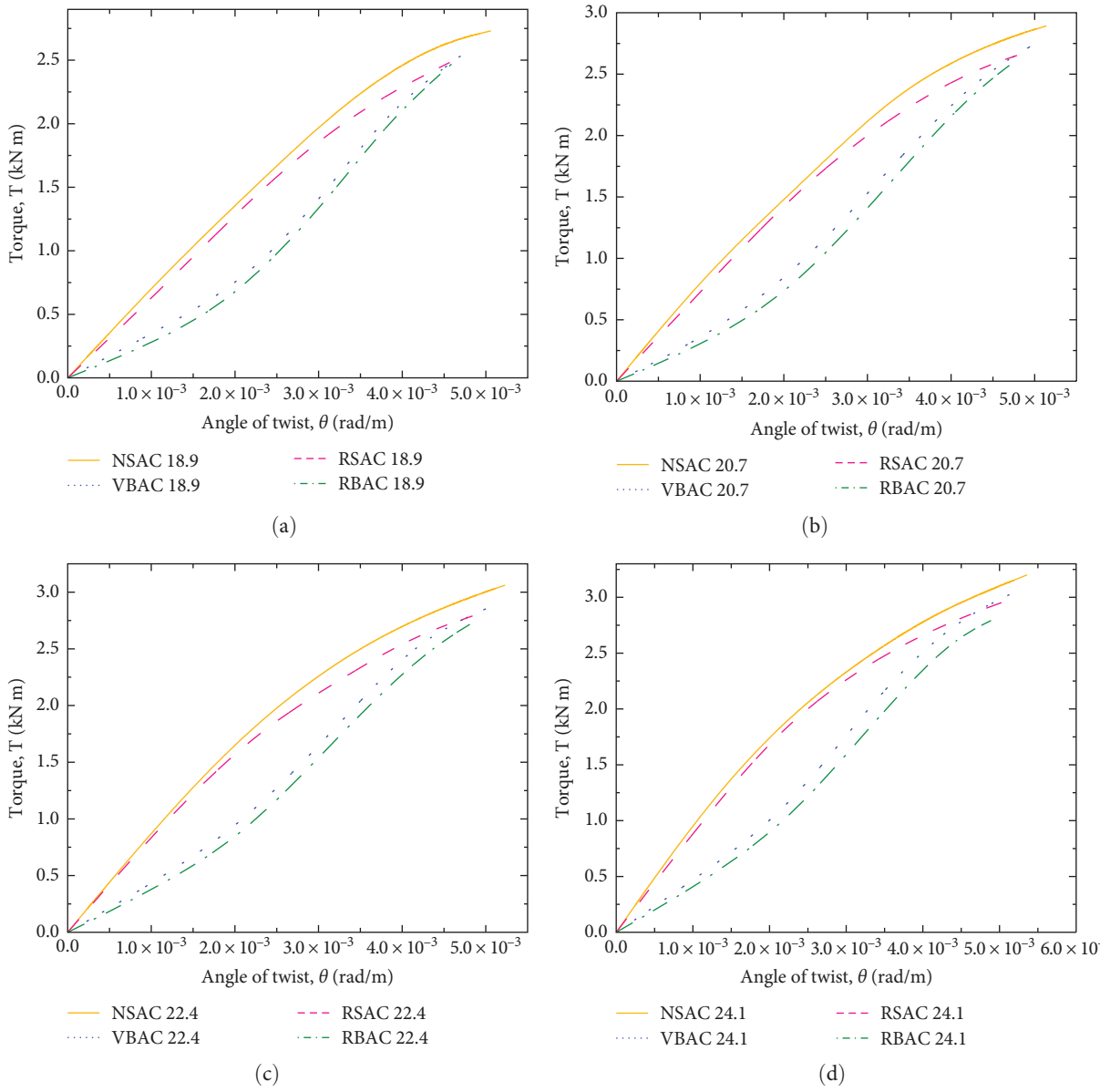

Figure 6: Torque vs. twisting curves for different target strength with different coarse aggregate: (a) for 18.9 MPa, (b) for 20.7 MPa, (c) for 22.4 MPa, and (d) for 24.1 MPa concrete.

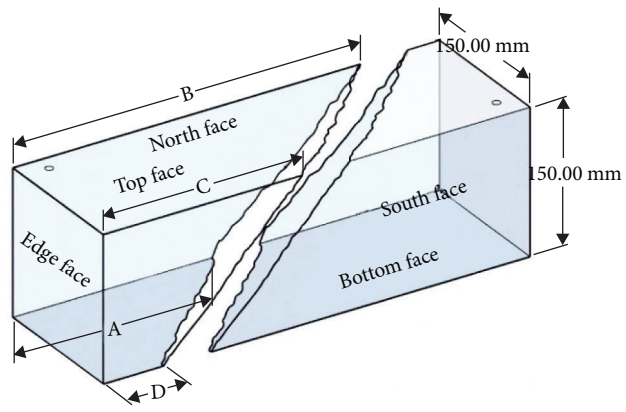

Figure 7: Three-dimensional schematic diagram of crack orientation and positions.

$$T = 1.35 f_{ctd}\, S. \tag{4}$$

S in Equation (4) is the shape factor, and for rectangular section, may be taken as $y^2\, x/3$. x and y are long and short sides of the rectangle.

f_{ctd} = axial tensile strength of concrete and may be considered as $f_{ctd} = 0.35(\sqrt{f_c'})$;

f'_c = compressive strength of concrete.

Hsu et al. [51] discovered that when subjected to pure torsion, plain-concrete beams failed by bending. The idea postulated that failure would occur when the tensile stresses generated by a 45° bending component of the torque reached a reduced value of modulus of rupture at wider face of the beam. According to this theory, ultimate torque of plain concrete members can be expressed as in following equation:

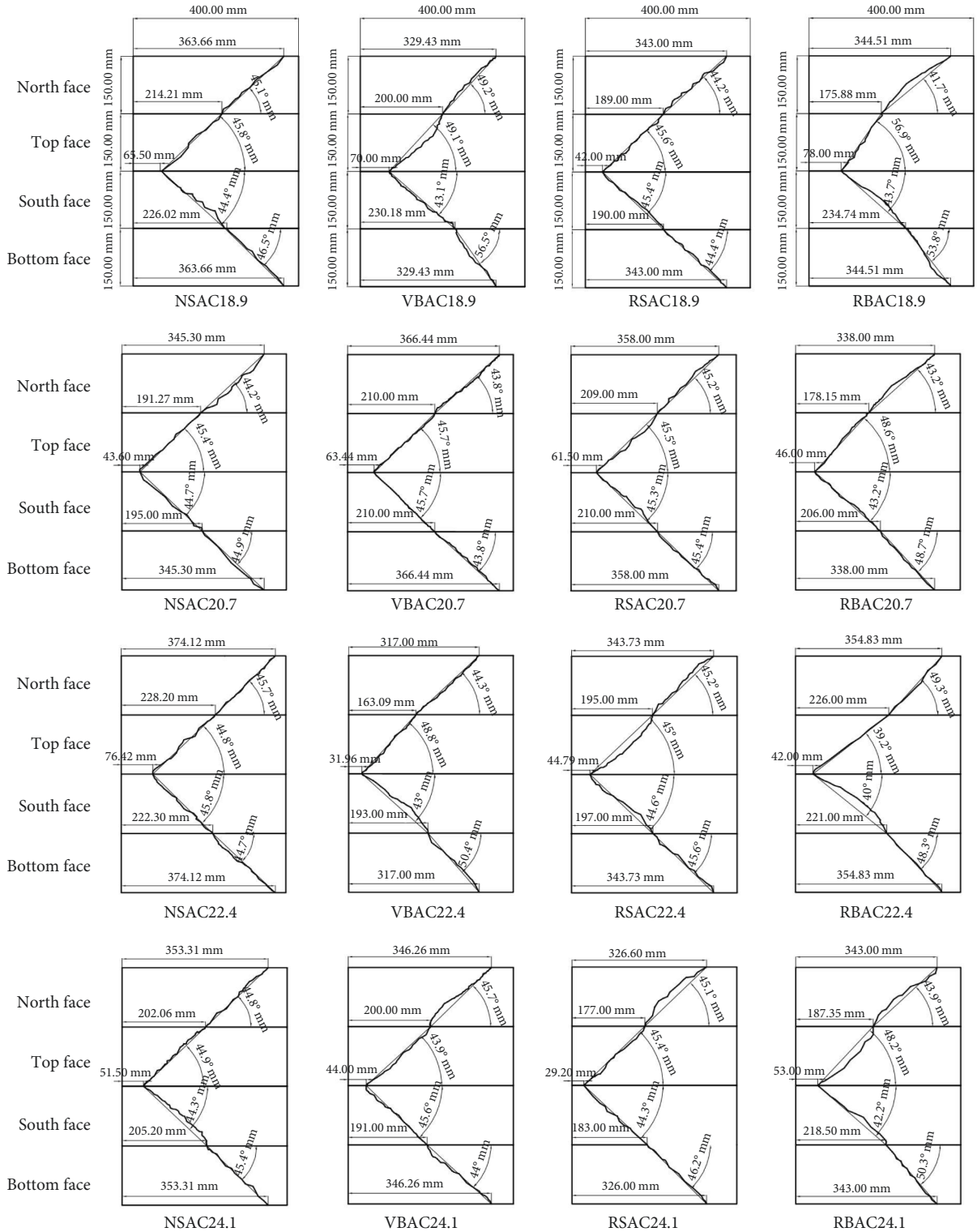

Figure 8: Crack orientation and locations for all beams.

$$T = x^2 y/3^{*}0.85\left(7.5\sqrt{f_c'}\right). \quad (5)$$

Here, $7.5\sqrt{f_c'}$ represents modulus of rupture of concrete.

Table 7 displays the estimated torsional capacity of these five models along with the actual ultimate torque obtained from the testing scheme. The errors for each data set and the root-mean-square errors (RMSE) for each model and for each concrete type are also presented in Table 7. All models underestimated the experimental results for all types of concrete except for VBAC, which had the lowest experimental torsional capacity. As the prediction from skew bending

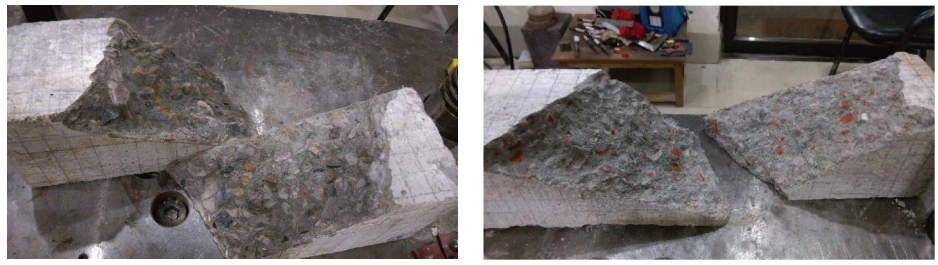

(a) (b)

Figure 9: Typical crack surface for (a) NSAC and (b) VBAC beams.

Table 7: Comparison of available torsional model with experimental torque.

Concrete type	Experimental torque (kN m)	Elastic theory (kN m)	Error (kN m)	Plastic theory (kN m)	Error (kN m)	Space truss (kN m)	Error (kN m)	TS 500 Turkish (kN m)	Error (kN m)	Skew bending (kN m)	Error (kN m)
NSAC18.9	2.731	2.612	−0.119	2.615	−0.116	1.307	−1.424	2.365	−0.366	2.778	0.047
NSAC20.7	2.893	2.731	−0.162	2.733	−0.16	1.367	−1.526	2.472	−0.421	2.904	0.011
NSAC22.4	3.062	2.847	−0.215	2.85	−0.212	1.425	−1.637	2.577	−0.485	3.028	−0.034
NSAC24.1	3.201	2.964	−0.237	2.966	−0.235	1.483	−1.718	2.682	−0.519	3.152	−0.049
RMSE			0.189		0.186		1.58		0.451		0.038
Ranking			3rd		2nd		5th		4th		1st
VBAC18.9	2.592	2.48	−0.112	2.483	−0.109	1.241	−1.351	2.245	−0.347	2.638	0.046
VBAC20.7	2.734	2.588	−0.146	2.59	−0.144	1.295	−1.439	2.342	−0.392	2.752	0.018
VBAC22.4	2.879	2.689	−0.19	2.692	−0.187	1.346	−1.533	2.434	−0.445	2.86	−0.019
VBAC24.1	3.024	2.786	−0.238	2.788	−0.236	1.394	−1.63	2.521	−0.503	2.963	−0.061
RMSE			0.178		0.176		1.492		0.426		0.040
Ranking			3rd		2nd		5th		4th		1st
RSAC18.9	2.554	2.468	−0.086	2.47	−0.084	1.235	−1.319	2.234	−0.32	2.625	0.071
RSAC20.7	2.685	2.575	−0.11	2.577	−0.108	1.289	−1.396	2.33	−0.355	2.738	0.053
RSAC22.4	2.831	2.673	−0.158	2.676	−0.155	1.338	−1.493	2.42	−0.411	2.843	0.012
RSAC24.1	2.967	2.769	−0.198	2.772	−0.195	1.386	−1.581	2.506	−0.461	2.945	−0.022
RMSE			0.145		0.142		1.451		0.390		0.046
Ranking			3rd		2nd		5th		4th		1st
RBAC18.9	2.482	2.451	−0.031	2.453	−0.029	1.227	−1.255	2.219	−0.263	2.607	0.125
RBAC20.7	2.594	2.557	−0.037	2.559	−0.035	1.28	−1.314	2.314	−0.28	2.719	0.125
RBAC22.4	2.716	2.655	−0.061	2.658	−0.058	1.329	−1.387	2.403	−0.313	2.824	0.108
RBAC24.1	2.793	2.748	−0.045	2.751	−0.042	1.376	−1.417	2.488	−0.305	2.923	0.13
RMSE			0.045		0.042		1.345		0.291		0.122
Ranking			2nd		1st		5th		4th		3rd

theory was always higher than all other models, its prediction was also closest to the experimental results except for VBAC. The accuracy of predictions using the plastic theory, the elastic theory, the TS500 Turkish theory, and the ACI space truss analogy decreased in that order. The utilization of various stress levels at which cracks in concrete begin to appear under torsional stress is the main cause of the variations in predictions made by these models. Elastic and TS500 Turkish theory use tensile strength as the stress in concrete when cracks begin. Plastic theory incorporates concrete properties of the plastic range and considers $6\sqrt{f_c'}$ as cracking stress. ACI space truss analogy conservatively considers $4\sqrt{f_c'}$ as the maximum tensile stress for cracks to start. And for skew bending theory, this is set as $7.5\sqrt{f_c'}$, the modulus of rupture of concrete. Accordingly, prediction from skew bending theory was highest and the ACI space truss analogy was lowest.

For the case of RBAC, predictions from skew bending theory were actually higher than the experimental results. However, other models underpredicted the experimental results. For RBAC, considering RMSE, the predicted capacity by plastic theory was closest to the experimental results. For all types of concrete, the greatest discrepancy between experimental results and the predicted capacity was found for the case of ACI space truss theory. Skew bending theory may be employed to conservatively predict the torsional capacity of plain concrete made from all types of aggregate except RBA.

6. Conclusion

In this work, a comprehensive testing scheme was carried out to examine and compare the torsional behavior of concrete formed from crushed clay bricks and recycled brick concrete as coarse aggregate. For this, concrete with target strength of 18.9, 20.7, 22.4, and 24.1 MPa were prepared with four different types of coarse aggregate namely natural stone, crushed clay brick, recycled stone, and recycled brick aggregate concrete. Cylinder (Ø 100 mm× 200 mm) and beam (150 mm× 150 mm × 400 mm) specimens were made from those concretes. Cylinder samples were tested to measure compressive strength, splitting tensile strength, density, porosity, and absorption of respective concrete. Beam samples were subjected to pure torsion up to failure to observe ultimate torque and maximum twisting angle as well as torque vs. twisting angle behavior. Based on these experimental results and analysis following conclusions may be stated:

(1) Crack due to torque and its angle with surface for NSAC, RSAC was found to remain close to 45° but for VBAC and RBAC, crack angle varied between wide range of 39° and 56°. Crack surface of VBAC and RBAC was relatively smooth compared to NSAC and RSAC. The later two had rough surface with protruding aggregate distributed over the surface.

(2) All beams failed with a loud noise, but for VBAC and RBAC beams the noise at failure was much louder compared to the NSAC and RSAC beams.

(3) For a given goal strength, NSAC had the highest ultimate torque, followed in descending order by VBAC, RSAC, and RBAC. For VBAC, the maximum torque was roughly 95% of that of NSAC. Whereas for RBAC, maximum torque was between 87% and 90% of that of NSAC. The initial slope of torque vs. angle of twist curves of VBAC and RBAC was only 47%–52% of that of NSAC. VBAC always had a lower initial slope than RSAC, but the ultimate torque for VBAC was found to be higher than that of RSAC.

(4) Torsional toughness of VBAC was 68%–72% of that of NSAC. On the other hand, torsional toughness of RBAC was only about 58%–61% of that of NSAC. Concrete built with VBA and RBA requires significantly less energy to fail in torsion compared to equivalent concrete made from NSA.

(5) Torsional strength prediction by five widely used models, namely, elastic theory, plastic theory, the ACI code space truss analogy method, the Turkish Standard TS500, and skew bending theory were compared to the experimental results. It was found that, except for one instance (Table 6), in general, all models underestimate the torsional strength of concrete prepared from the four types of aggregates utilized in this work. As per RMSE for VBAC beams, the ultimate torque estimation made by skew bending theory was shown to be the most accurate. For RBAC beams, prediction by the plastic method was found to be nearest to the experimental findings.

Data Availability

The experimental data used to support the findings of this study are available from the corresponding author upon request.

Conflicts of Interest

The authors declare that they have no conflicts of interest.

Acknowledgments

The work was funded by Bangladesh University of Engineering and Technology for graduate level research of Mr. Md. Ashraful Alam.

References

[1] B. Wang, L. Yan, Q. Fu, and B. Kasal, "A comprehensive review on recycled aggregate and recycled aggregate concrete resources," *Conservation and Recycling*, vol. 171, Article ID 105565, 2021.

[2] N. R. Mohanta and M. Murmu, "Alternative coarse aggregate for sustainable and eco-friendly concrete—a review," *Journal of Building Engineering*, vol. 59, Article ID 105079, 2022.

[3] M. Etxeberria, A. R. Marí, and E. Vázquez, "Recycled aggregate concrete as structural material," *Materials and Structures*, vol. 40, no. 5, pp. 529–541, 2007.

[4] S. N. Chinnu, S. N. Minnu, A. Bahurudeen, and R. Senthilkumar, "Recycling of industrial and agricultural wastes as alternative coarse aggregates: a step towards cleaner production of concrete," *Construction and Building Materials*, vol. 287, Article ID 123056, 2021.

[5] S. I. Ahmad, Z. B. Ahmed, and T. Ahmed, "Feasibility of sludge generated in water-based paint industries as cement replacement material," *Case Studies in Construction Materials*, vol. 16, Article ID e01119, 2022.

[6] S. I. Ahmad and M. S. Rahman, "Mechanical and durability properties of induction-furnace-slag-incorporated recycled aggregate concrete," *Advances in Civil Engineering*, vol. 2018, Article ID 3297342, 11 pages, 2018.

[7] W. Xing, V. W. Y. Tam, K. N. Le, J. L. Hao, and J. Wang, "Life cycle assessment of recycled aggregate concrete on its environmental impacts: a critical review," *Construction and Building Materials*, vol. 317, Article ID 125950, 2022.

[8] B. Estanqueiro, J. D. Silvestre, J. de Brito, and M. D. Pinheiro, "Environmental life cycle assessment of coarse natural and recycled aggregates for concrete," *European Journal of Environmental and Civil Engineering*, vol. 22, no. 4, pp. 429–449, 2016.

[9] T. U. Mohammed, A. Hasnat, M. A. Awal, and S. Z. Bosunia, "Recycling of brick aggregate concrete as coarse aggregate," *Journal of Materials in Civil Engineering*, vol. 27, no. 7, 2015.

[10] S. Roy, S. I. Ahmad, M. S. Rahman, and M. Salauddin, "Experimental investigation on the influence of induction furnace slag on the fundamental and durability properties of virgin and recycled brick aggregate concrete," *Results in Engineering*, vol. 17, Article ID 100832, 2023.

[11] M. S. Islam and M. A. A. Siddique, "Behavior of low grade steel fiber reinforced concrete made with fresh and recycled brick aggregates," *Advances in Civil Engineering*, vol. 2017, Article ID 1812363, 14 pages, 2017.

[12] F. M. Khalaf, "Using crushed clay brick as coarse aggregate in concrete," *Journal of Materials in Civil Engineering*, vol. 18, no. 4, pp. 518–526, 2006.
[13] F. Debieb and S. Kenai, "The use of coarse and fine crushed bricks as aggregate in concrete," *Construction and Building Materials*, vol. 22, no. 5, pp. 886–893, 2008.
[14] S. I. Ahmad and S. Roy, "Creep behavior and its prediction for normal strength concrete made from crushed clay bricks as coarse aggregate," *Journal of Materials in Civil Engineering*, vol. 24, no. 3, pp. 308–314, 2012.
[15] S. I. Ahmad and M. A. Hossain, "Water permeability characteristics of normal strength concrete made from crushed clay bricks as coarse aggregate," *Advances in Materials Science and Engineering*, vol. 2017, Article ID 7279138, 9 pages, 2017.
[16] C. Joh, I. Kwahk, J. Lee, I.-H. Yang, and B.-S. Kim, "Torsional behavior of high-strength concrete beams with minimum reinforcement ratio," *Advances in Civil Engineering*, vol. 2019, Article ID 1432697, 11 pages, 2019.
[17] A. Deifalla, "Torsion design of lightweight concrete beams without or with fibers: a comparative study and a refined cracking torque formula," *Structures*, vol. 28, pp. 786–802, 2020.
[18] T. T. C. Hsu, *Torsion of Structural Concrete—Behavior of Reinforced Concrete Rectangular Members Torsion of Structural Concrete*, pp. 261–306, American Concrete Institute SP-18, Detroit, 1968.
[19] A. E. McMullen and B. V. Rangan, "Pure torsion in rectangular sections—a re-examination," *Journal of American Concrete Institute*, vol. 75, no. 10, pp. 511–519, 1978.
[20] N. Masne and S. Suryawanshi, "Analytical and experimental investigation of recycled aggregate concrete beams subjected to pure torsion," *International Journal of Engineering*, vol. 35, no. 10, pp. 1959–1966, 2022.
[21] K. J. N. S. Nitesh, S. V. Rao, and P. R. Kumar, "An experimental investigation on torsional behaviour of recycled aggregate based steel fiber reinforced self compacting concrete," *Journal of Building Engineering*, vol. 22, pp. 242–251, 2019.
[22] H. Ju and A. Serik, "Torsional strength of recycled coarse aggregate reinforced concrete beams," *Civil Engineering*, vol. 4, no. 1, pp. 55–64, 2023.
[23] ASTM, "Standard specification for portland cement, ASTM C150/C150M-20," West Conshohocken, PA, USA, 2020.
[24] ASTM, "Standard specification for concrete aggregates, ASTM C33/C33M-18," West Conshohocken, PA, USA., 2018.
[25] ASTM, "Standard test method for bulk density ("unit weight") and voids in aggregate, ASTM C29/C29M-17a," West Conshohocken, PA, USA, 2017.
[26] ASTM, "Standard test method for relative density (specific gravity) and absorption of fine aggregate, ASTM C128-15," West Conshohocken, PA, USA, 2015.
[27] Bangladesh Standards and Testing Institution (BSTI), "Specification for common building clay bricks BDS 208: 2002," Dhaka, Bangladesh, 2007.
[28] I. Kesegić, I. Netinger, and D. Bjegović, "Recycled clay brick as an aggregate for concrete: overview," *Technical Gazette*, vol. 15, pp. 35–40, 2008.
[29] S. Kenai, "Recycled aggregate," in *Waste and Supplementary Cementitious Materials in Concrete*, pp. 79–120, Woodhead Publishing Series in Civil and Structural Engineering, 2018.
[30] ASTM, "Test method for relative density (specific gravity) and absorption of coarse aggregate," West Conshohocken, PA, USA, 2018.
[31] ASTM, "Standard test method for sieve analysis of fine and coarse aggregates, ASTM C136/C136M-19," West Conshohocken, PA, USA, 2019.
[32] ASTM, "Standard test method for resistance to degradation of small-size coarse aggregate by abrasion and impact in the los angeles machine, ASTM C131," West Conshohocken, PA, USA, 2019.
[33] BSI, "Testing aggregates part 1: methods for determination of particle size and shape BS 812-1," London, 1991.
[34] American Concrete Institute (ACI), "Standard practice for selecting proportions for normal, heavyweight and mass concrete, ACI 211.1-91," Famington Hills, MI., USA, 2002.
[35] ASTM, "Standard test method for slump of hydraulic-cement concrete, ASTM C143/C143M-20," West Conshohocken, PA, USA, 2020.
[36] Z. P. Bažant, S. Şener, and P. C. Prat, "Size effect tests of torsional failure of plain and reinforced concrete beams," *Materials and Structures*, vol. 21, no. 6, pp. 425–430, 1988.
[37] K. Kirane, K. D. Singh, and Z. P. Bažant, "Size effect in torsional strength of plain and reinforced concrete," *ACI Structural Journal*, vol. 113, no. 6, pp. 1253–1262, 2016.
[38] Z. P. Bažant and S. Şener, "Size effect in torsional failure of concrete beams," *Journal of Structural Engineering*, vol. 113, no. 10, pp. 2125–2136, 1987.
[39] ASTM, "Standard test method for compressive strength of cylindrical concrete specimens, ASTM C39/C39M-21," West Conshohocken, PA, USA., 2021.
[40] ASTM, "Standard test method for splitting tensile strength of cylindrical concrete specimens, ASTM C496/C496M-17," West Conshohocken, PA, USA, 2017.
[41] ASTM, "Standard test method for density, absorption and voids in hardened concrete, ASTM C642," West Conshohocken, PA, USA, 2021.
[42] R. Bitter, T. Mohiuddin, and M. Nawrocki, *LabVIEW: Advanced Programming Techniques*, CRC Press, 2006.
[43] T. T. C. Hsu, *Torsion of Structural Concrete-Plain Concrete Rectangular Section*, pp. 206–238, ACI Special Publication, 1968.
[44] N. Arthur, D. Darwin, C. Dolan, A. H. Nilson, and C. W. Dolan, *Design of Concrete Structures*, McGraw-Hill Science, Engineering & Mathematics, 2009.
[45] J. N. Goodier and S. Timoshenko, *Theory of Elasticity*, McGraw-Hill, 1970.
[46] E. P. Popov, *Engineering Mechanics of Solids*, Prentice-Hall, 1990.
[47] A. H. Nilson, "Design implications of current research on high strength concrete, high strength concrete (ACI SP-87)," pp. 85–118, 1985.
[48] American Concrete Institute (ACI), "Building code requirements for reinforced concrete, ACI 318-19," Famington Hills, MI., USA, 2019.
[49] TSI (Turkish Standards Institution), "Requirements for design and construction of reinforced concrete structures, TS 500," Ankara, 2000.
[50] T. T. C. Hsu, *Torsion of Reinforced Concrete*, Van Nostrand Reinhold Company, 1984.
[51] T. T. C. Hsu and Y. L. Mo, "Softening of concrete in torsional members-theory and tests," *ACI Journal*, vol. 82, no. 3, pp. 290–303, 1985.